Egypt. J. Chem. **Vol. 63,** No. 4, pp. 1219 - 1240 (2020)

Egyptian Journal of Chemistry
http://ejchem.journals.ekb.eg/

Novel Simple Modification of Chitosan as Adsorptive Agent for Removal of Cr^{6+} from Aqueous Solution

Mohamed N. M. Ismail[1], Ahmed El Nemr[1]*, El Sayed H. El Ashry[2]*, Hamida Abdel Hamid[2]

[1] Marine Pollution Department, Environment Division, National Institute of Oceanography and Fisheries, Kaye1t Bey, El-Anfoushy, Alexandria, Egypt.

[2] Department of Chemistry, Faculty of Science, Alexandria University, Alexandria, Egypt.

CHITOSAN grafted crotonaldehyde (CGC) by nucleophilic addition reaction of the amine group with α,β-unsaturated aldehyde was achieved by simple method using Lewis acid FeCl3.6H2O or ZrOCl2.8H2O as a catalyst. The product has been extensively characterized using FTIR, TGA, SEM, and EDX. The CGC was used for removal of hexavalent chromium from its aqueous solution. Batch experiment was tested using different contact times and initial Cr^{6+} ion concentrations under acidic condition (pH 1.5). Isotherm studies were achieved using variable models (Langmuir, Freundlich, and Tempkin) which showed a 10-fold greater uptake (434.78 mg/g) for modified chitosan over non-modified chitosan. The kinetics of Cr^{6+} adsorption by CGC followed the pseudo-second order model. This study proved that the CGC is a promising material for the treatment of wastewater containing Cr^{6+} ions.

Keywords: Chitosan, Crotonaldehyde, Cr6+ removal, Ferric chloride, Zirconyl chloride

Introduction

Recent trends in human growth and their subsequent needs of everyday life have prompted a boom in the development of all industrial sectors from basic food and water processing to fancy cars and other high-end gadgets production. However, one of the cons of all this is that it puts a huge load on the abundant natural resources and increases pollution levels which lead to catastrophic effects on the environment and human health [1]**.** In wastewater treatment technology, removal of coexisting heavy metal ions is challenging. However, these toxic ions are difficult to be removed and need certain conditions (pH, temperature, salinity) to complete removal of toxic pollutants [2]. There are dangerous substances (heavy metals) that pollute the environment like as dyes on industrial scale [3]. Cr^{6+} is more hazardous by comparison with Cr^{3+} due to its highly toxic and carcinogenic nature [4]. The permissible concentrations of Cr^{6+} in drinking water have been set as 0.05 ppm according to WHO guidelines [5]. Cr^{6+} in wastewater is fundamentally found from electroplating, leather tanning, pigment manufacturing and mining industries [6]. Conventional methods for the removal of Cr^{6+} from water include solvent extraction [7], mechanical filtration [8,9], Chemical precipitation [9,10], nano filtration [11], redox reaction [12], photocatalytic reduction [13] and adsorption [9,14-16].

The removal of different pollutants using adsorption technique is the most important and efficient conventional methods of wastewater treatment because of its simplicity, sludge free operation, easiness in handling, availability of various adsorbents, regenerative and high efficient for removal of lower concentration levels [17-

*Corresponding author e-mail: ahmedmoustafaelnemr@yahoo.com
Received 26/03/2019; Accepted 02/10/2019
DOI: 10.21608/ejchem.2019.11157.1716

19]. Many adsorbent types have been developed and reported for treatment of different types of wastewater [20-22].

Recently, bio-based adsorbents such as cellulose, chitosan, and biomass have found great attentions due to their abundancy (i.e. natural resource), non-toxic nature [23]. So many researchers use chemically modified natural polymer to remove Cr^{6+} from polluted water. Chitosan (Cs) is prepared from the de-acetylation of the natural biopolymer chitin, found in crustaceous shells, insects, and fungal cell walls, Cs consists of β-(1→4)-2-acetamido-2-deoxy-D-glucose and contains high contents of amino and hydroxyl groups, which prefer the modification of this biopolymer and the introduction of new functional groups [24]. Presence of abundant amino and hydroxyl functional groups in the structure of chitosan enables modification via cross-linking to yield materials with non-toxic, biodegradable, and biocompatible properties. Therefore modifying chitosan using either physical or chemical processes have been received increasing interests in order to increase its capabilities to remove selective heavy metals. Chemical modification is the application of chemical treatment on chitosan, which improves its stability in acidic media and increases the active side to selective adsorption of heavy metals by using different methods to modify chitosan such as crosslinking, grafting, carboxymethylation, and blending [25].

In this paper, a new functional adsorbent from chitosan by grafting with crotonaldehyde was synthesized by nucleophilic addition reaction of amino group of chitosan to the α,β-unsaturated aldehyde using Lewis acids such as $FeCl_3$ or $ZrOCl_2$. The modified chitosan was characterized by FTIR, TGA, EDX and SEM. The synthesized adsorbent was tested for Cr^{6+} adsorption. The adsorption thermodynamic and kinetics were studied.

Experimental

Material and instrumentation

Chitosan (oxford laboratory reagent, deacetylation 93%, made in India), crotonaldehyde (Cambrian Chemicals), acetonitrile (Carbon Group, Ringaskiddy, Cork, Ireland), iron(III) chloride 6 hydrated (Nice Chemicals(p) LTD, Kerala, India), zirconyl chloride octahydrate (ACROS ORGANIC, New jersey, USA). All chemicals were used as submitted by the chemical companies.

Shaker (A JS shaker, JSOS-500), pH-meter JENCO (6173), Fourier transform infrared spectrometer (FTIR: Bruker Vertex 70, Platinum ATR), Scanning electron microscope (SEM: LEO, 1450 VP), Digital spectrophotometer (Analytic Jena (SPEKOL1300 UV/Visible spectrophotometer) with matched glass cells of 1cm optical path length.

Preparation of chitosan grafted crotonaldehyde (CGC)

Crotonaldehyde (13.29 mL) was added to a mixture of chitosan (5.0 g) and different amount of iron(III)chloride hydrated or zirconyl chloride as Lewis acid catalyst using acetonitrile (100 mL) under vigorous stirring at reflux for 24 h. The reaction mixture was left to cool, poured onto ice water (250 mL), and the precipitated was filtered, washed with distilled water and dried for 24 h at 60 °C in an oven. The catalyst amount used and yield weight of the modified chitosan are summarized in Table 1.

Adsorption study

A stock solution of hexavalent chromium (1000 mg L^{-1}) was prepared by dissolving of $K_2Cr_2O_7$ (2.8289 g) in distilled water (1000 mL), and this solution was diluted to different proposed concentration for further removal application. The standard curve was obtained by preparation of different concentrations ranged between 10 and 70 mg L^{-1} by dilution from the stock solution.

A batch adsorption experiments were employed to evaluate the adsorption capability and thermodynamic and kinetic parameters of synthesized chitosan grafted crotonaldehyde (CGC). A series of 250 mL reagent bottles containing 100 mL of different concentrations of Cr^{6+} ions solution and different amounts of CGC were shaken at 200 rpm for a certain time. The pH of the studied wastewater was controlled by addition of few drops of either 0.1M HCl or 0.1M NaOH. About 0.1 mL of the solution in the reagent bottles was then separated from the adsorbent, and the concentration of Cr^{6+} was detected at different interval times and at the equilibrium. Spectrophotometer was used to determine the degree of the violet color Cr^{6+} ions concentration at λ_{max} 540 nm using 1,5-diphenylcarbazide as reagent. The concentration of chromium

in the initial, interval times and equilibrium solutions was determined by spectrophotometer. The adsorption capacities at equilibrium were calculated by using the following equation (1):

$$q_e = \frac{(C_0 - C_e)}{W} \times V \qquad (1)$$

where q_e (mg g^{-1}) is the amount of adsorbent (Cr^{6+}) removed at equilibrium; C_0 and C_e are the chromium initial and equilibrium concentrations (mg L^{-1}), respectively; V (L) is the solution volume and W is the mass of CGC (g) [1].

The effect of solution pH on the percentage of removal was studied using pH ranged from 1.5 to 9.0 and 250 mg CGC of 100 mL volume containing 100 mg L^{-1} concentration Cr^{6+} at room temperature.

The percentage of removal was calculated by equation (2):

$$Removal\ \% = \left(\frac{C_0 - C_t}{C_0}\right) \times 100 \qquad (2)$$

where C_0 and C_t are the initial and interval chromium concentrations at t time in the liquid phase (mg L^{-1}), respectively.

The adsorption isotherms and kinetic studies were achieved by shaking (200 rpm) of CGC (0.10, 0.15, 0.20, 0.25, and 0.30 g) individually with 100 mL of Cr^{6+} solution (50, 75, 100, 150 and 200 mg L^{-1}) at room temperature (25 ± 2 °C) at pH (1.5). The clear samples (0.10 mL) at equilibrium time were analyzed using spectrophotometer for the remaining amount of Cr^{6+} ions concentration in the solutions. All the experiments were replicated and the mean value of the results were summarized. A deviation less than ± 3% was observed in the adsorption experiments.

Results and Discussion

The reaction of chitosan with crotonaldehyde in acetonitrile in the presence of $FeCl_3$ or $ZrOCl_2$ as Lewis acid catalyst leads to formation of the chitosan grafted crotonaldehyde (CGC) in almost quantitative yield (Scheme 1). The CGC obtained was studied using FTIR, TGA and SEM.

Characterization of CGC and CGC_{ads}-Cr^{6+}

Thermal gravimetric analysis (TGA)

The TGA was performed on the chitosan and CGC to detect their degradation behavior [26]. Each sample was heated from 25 to 800 °C under flow of N_2 atmosphere. The TGA of chitosan (Fig. 1a) showed a first degradation at about 66 °C with weight loss percentage of 10.54% and second degradation at about 302 °C with weight loss percentage of 74.30%. There is no further decomposition of chitosan above this temperature. The TGA of CGC (Fig. 1b) showed initial degradation at 65.94 °C with weight loss percentage of 17.5%, then a second degradation occurred at 287 °C with weight loss percentage of 37.99% and the last degradation occurred at 426.73 °C with weight loss percentage of 23.06%, which may reflect a slightly more stability for CGC than chitosan. The decomposition temperature at ca. 426 obtained from TGA result for CGC is related to breaking the grafted CGC units

EDX-analysis

The EDX analysis of CGC and chromium adsorbed by CGC samples are reported in Table 2 and Fig. 2. Fig. 2a shows the absence of chromium peak before the removal experiment while Fig. 2b shows the presence of new peak for Cr in the sample used for chromium solution treatment. The presence of peaks for Fe and Cl are due to the use of the $FeCl_3$ as a catalyst. Increasing in the Cl% in the investigated sorbents could be attributed to the amount of HCl used for the solution pH adjustment. The EDX analysis of CGC_{ads}-Cr^{6+} sample proved the presence of about 15.78% of sample weight.

Scanning electron microscope (SEM) study

Scanning electron microscopy (SEM) is the advance technique, that used for detailed examination of the microscopic organisms and provide an additionally opportunity for in depth analysis of seed coat texture and sculpturing, having significant importance to solve taxonomic problems at different levels [27]. In this study the morphology of CGC and CGC_{ads}-Cr^{6+} samples were characterized by SEM images as shown in Fig. 3. CGC image shows a porous surface morphology contained pores of different size and shapes (non-uniform holes) (Fig. 3a), which may be responsible for effective adsorption of Cr^{6+} ions. The SEM micrograph of CGC loaded with Cr^{6+} ions shows bright spots on non-uniform surface indicates the interaction of Cr^{6+} with the adsorbent (Fig. 3b). The SEM image of CGC_{ads}-Cr^{6+} sample shows almost complete disappear of

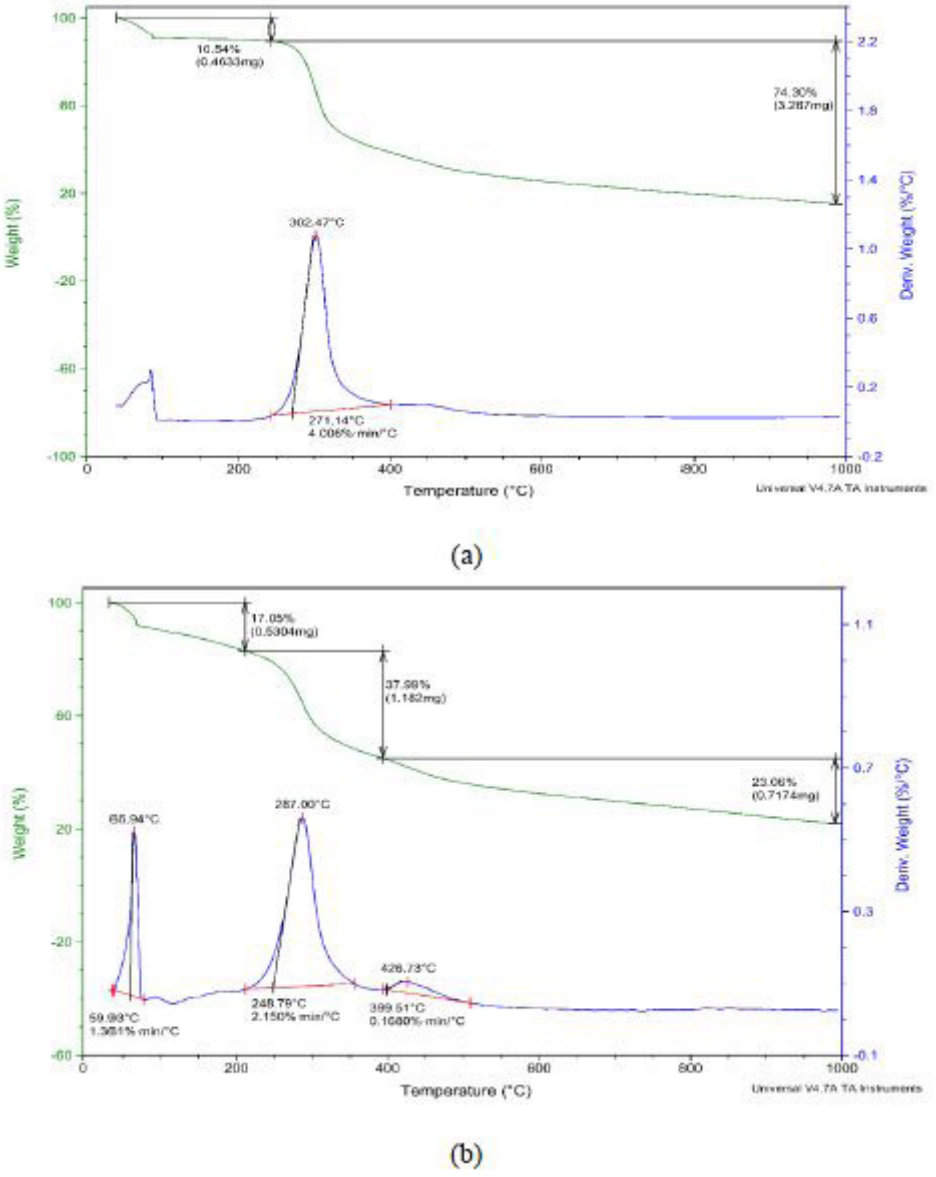

Fig. 1. Thermal gravimetric analysis of (a) chitosan and (b) CGC.

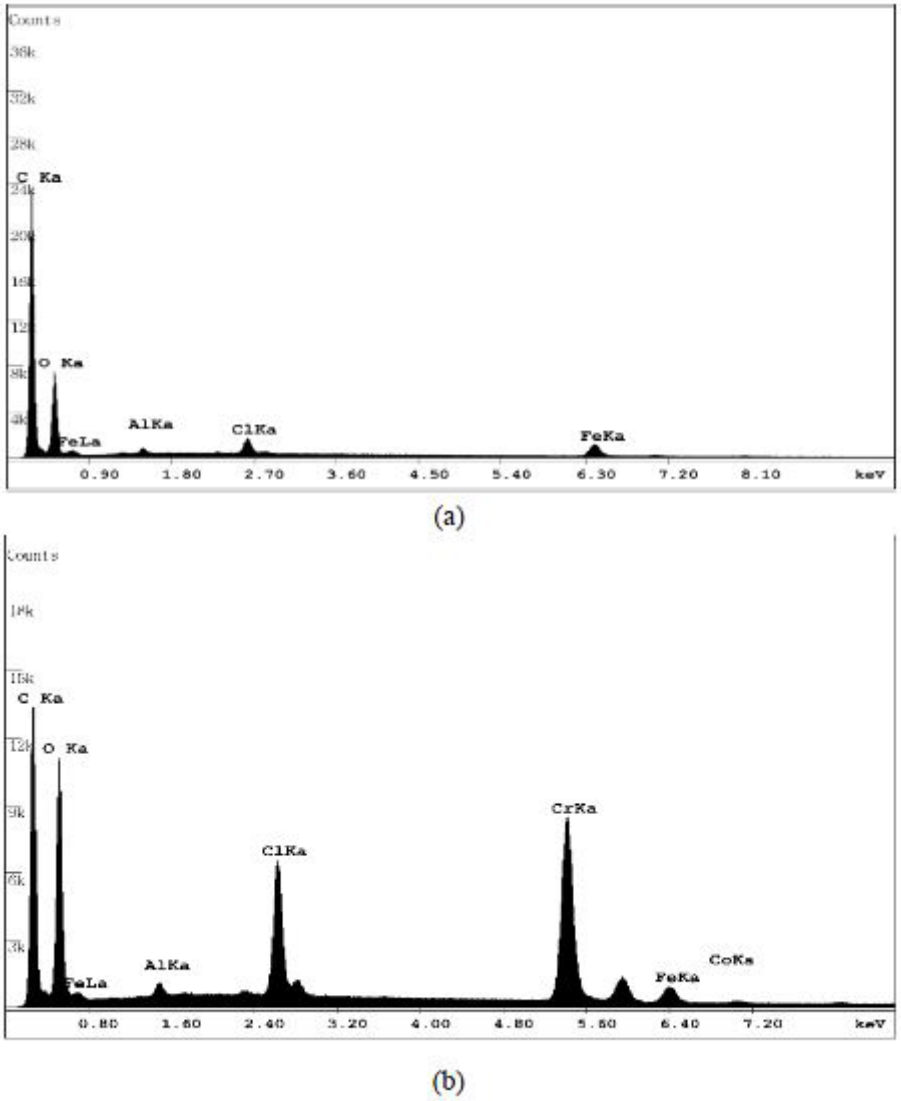

Fig. 2. (a) EDX spectra of CGC, (b) EDX spectra of Cr^{6+} adsorbed on CGC.

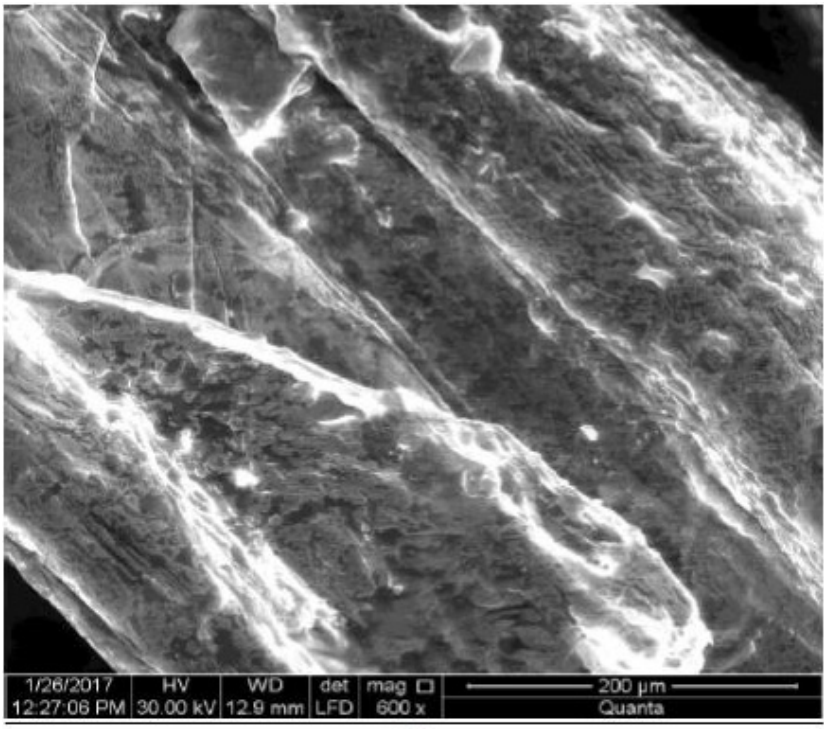

(a)

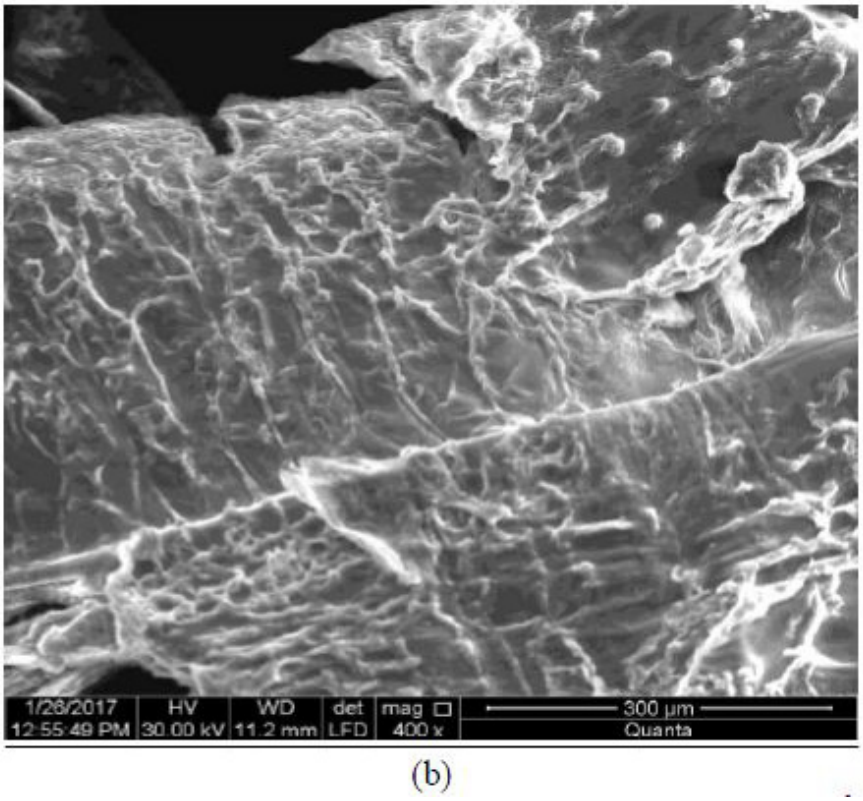

(b)

Fig. 3. (a) SEM image of CGC, (b) SEM image of CGC loaded with Cr^{6+}.

the surface pores, which reflect the high loaded of Cr^{6+} ions onto the CGC surface.

FTIR analysis

The surface functional groups of chitosan and its derivative were analyzed by Fourier transform infrared (FTIR) spectroscopy using Bruker model VERTEX 70 connected with platinum ATR unit model V-100 in the wave number range of 400-4000 cm^{-1}. Fig. 4 shows the FTIR spectra of chitosan and CGC obtained by $FeCl_3$ and $ZrOCl_2$ as catalysts. FTIR of chitosan, the characteristic bands were: the axial stretching of –OH and C-H groups at 3354 and 2870 cm^{-1}, respectively, C=O stretching band (amide I): 1645 cm^{-1}, N-H angular deformation at 1590 cm^{-1}, CH_3 symmetrical angular deformation at 1376 cm^{-1}, C-N amino axial deformation at 1322 cm^{-1}, besides the two characteristic polysaccharide angular deformation bands, 1062 and 1150 cm^{-1}. The FTIR spectra of CGC by $ZrOCl_2$ or $FeCl_3$ presented a strong adsorption bands at 1680 and 1713 cm^{-1} (for sample prepared by $FeCl_3$) and bands at 1656 and 1717 cm^{-1} (for sample prepared by $ZrOCl_2$) which represented the C=O and at the same time appearing of three peaks at about 2874, 2929 and 2963 cm^{-1} characteristic for the presence of CH_2 group. There are same peaks observed in the spectrum of nano-materials such as, metal based modified bentonites, zeolites etc that has significant applications in renewable energy [28,29] and The FTIR analysis proved the presence of the new C=O and CH_2 groups as a results of the nucleophilic addition reaction of NH_2 of chitosan to the α,β-unsaturated aldehyde of crotonaldehyde.

FTIR spectra of CGC with $FeCl_3$ before and after loaded with Cr^{6+} ions are shown in Fig. 5. The different in infrared bands before and after adsorption proved the success of adsorption process, which showed a very small shift (–3 cm^{-1}) in the band at 1680 cm^{-1} and appeared of new two bands at 1633 and 1521 cm^{-1} that indicated the formation of a complex with Cr^{6+} ions. These peaks may be reflect that the new group produced from the grafting of chitosan is responsible for the high efficiency of the CGC in the removal of Cr^{6+} ions from its water solution.

Effect of pH

The pH of solution is important factor that affect the heavy metals removal efficiency [4]. The variation of Cr^{6+} removal over CGC sample with different initial pH (1.5 up to 9.5) was studied and given in Fig. 6. It is clear that the CGC was more active in the acidic range and maximum removal percentage occurred at pH 1.5. The lowest removal percentage was reported for the alkaline medium (pH 9.5). The removal values decreased significantly with the increase in pH value from acidic to basic. At optimum sorption pH, the common species of Cr^{6+} ions in solution are $HCrO^{4-}$, $Cr_2O_7^{2-}$, $Cr_4O_{13}^{2-}$ and $Cr_3O_{10}^{2-}$, which could be adsorbed initially by higher electrostatical force nature at acidic pH 1-3. The surface of sorbent would also be surrounded by H_3O^+, which increase the Cr^{6+} interaction with binding sites of CGC greater attractive forces. By increasing pH to the basic value the overall surface charge on CGC became negative and adsorption of chromium decreased [30]. Also, it has been known that in the case of high chromium concentration, the $Cr_2O_7^{2-}$, ions precipitate at higher pH values [31].

CGC surface would be positively charged up to pH < 3, and heterogeneous in the pH range 3–6. Therefore, it should be negatively charged at pH higher than 7. Also, it should be mentioned that the form and valiancy of chromium ion are pH dependent and the adsorption process is chromium ion form dependent, therefore, the percentage of removal is highly dependent on solution pH.

Effect of initial Cr^{6+} concentration

The high initial concentration of pollutant is an important parameter to produce force to overcome the mass transfer resistance between the aqueous phase containing pollutant ions and the solid phase. Hence, a higher initial concentration of Cr^{6+} ions will increase the rate of adsorption. The results of percentage removal of Cr^{6+} ions at pH 1.5 were studied at initial chromium concentrations from 50 to 200 mg L^{-1} with different CGC doses (0.10 to 0.30 g L^{-1}) (Fig. 7). The results show that the Cr^{6+} removal percentage decreased as the initial concentration of Cr^{6+} increased. In the process of Cr^{6+} adsorption, first metal ions have to encounter the boundary layer effect and then diffuse from boundary layer film onto CGC surface and finally, it has to diffuse into the porous structure of the CGC. This phenomenon will need a relatively longer contact time.

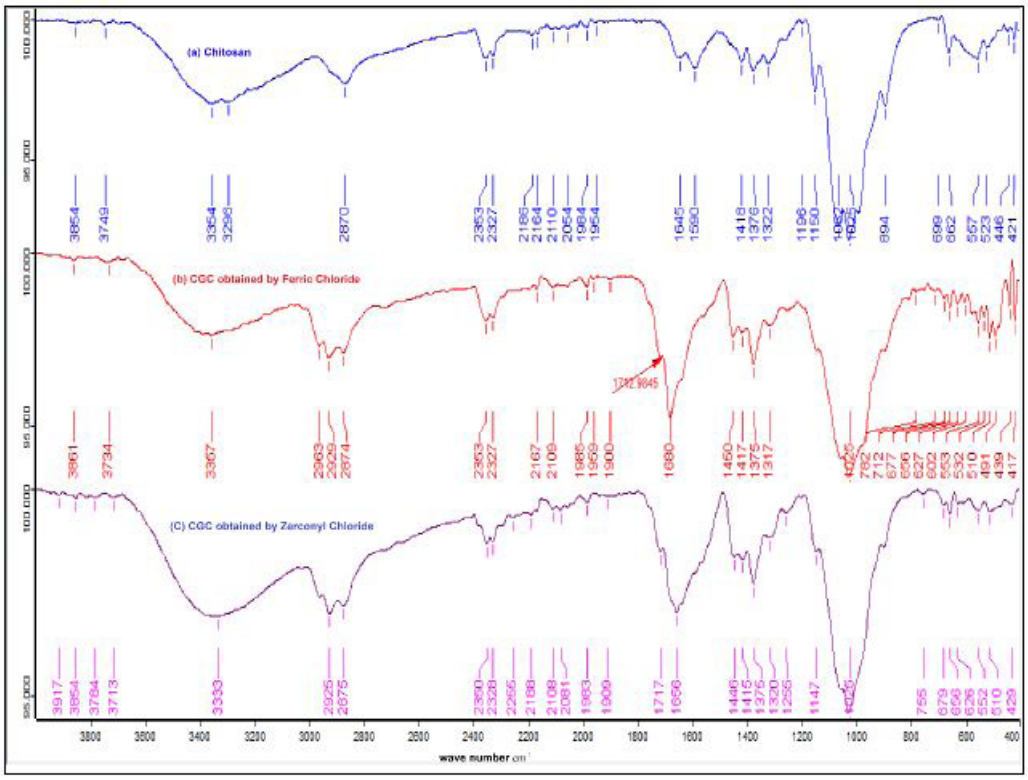

Fig. 4. FTIR (a) chitosan, (b) CGC by $FeCl_3$ catalyst, (c) CGC by $ZrOCl_2$ catalyst.

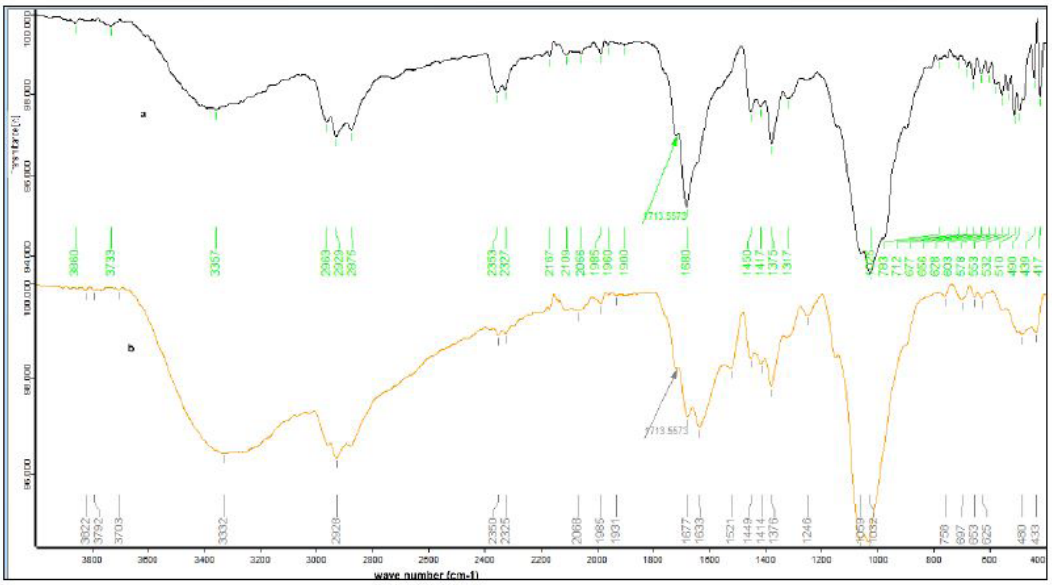

Fig. 5. FT-IR of (a) CGC obtained by $FeCl_3$ and (b) CGC obtained by $FeCl_3$ after loaded with Cr^{6+}.

Effect of contact time

The relation between adsorption of Cr^{6+} ions and contact time were studied and reported in Fig. 8. The removal percentage of Cr^{6+} ions at different initial chromium concentrations ranged from 50 to 200 mg L^{-1} at pH 1.5 were ranged between 68.88 and 98.99%. The equilibrium time was about 60 min and after that the removal percentage was more or less constant. Therefore, it can be concluded that the adsorption rate of Cr^{6+} ions over CGC was greater in the initial stages, then gradually decreased and remained almost constant after 60 min. The slow rate of Cr^{6+} ions adsorption after the first 15 min is probably occurred due to the electrostatic hindrance or repulsion between the adsorbed negatively charged Cr^{6+} onto the surface of CGC and the available anionic Cr^{6+} in solution as well as the slow pore diffusion of the Cr^{6+} ions into the bulk of the CGC dose. The major effect on the adsorption of Cr^{6+} by CGC will be the electrostatic interactions occurred due to the presence of highly acidic solution (pH 1.5), which control the adsorption process via the attraction and repulsion between CGC surface and Cr^{6+} ions.

Effect of adsorbent dose on metal adsorption

The effect of CGC dosage on the adsorption of Cr^{6+} ions from aqueous solutions was investigated using five different adsorbent concentrations (0.50 to 3.0 g L^{-1}) and five different initial chromium concentration (50 to 200 mg L^{-1}) at pH 1.5. The results indicated that the equilibrium concentration (C_e) of Cr^{6+} ion decreases with increasing CGC concentration for a given initial Cr^{6+} ion concentration. This results may be due to the fact that the higher sorbent doses provide the higher sorbent surface area and higher pore volume that will be available for metal ions adsorption.

Adsorption equilibrium isotherm models

Study of the adsorption isotherm models is important to describe the sorbate molecules fraction that are distribute at equilibrium between liquid and solid phases. Three adsorption isotherm models (Langmuir, Freundlich, and Tempkin isotherms) were applied for Cr^{6+} adsorption on CGC sample. The Langmuir model presumes that the adsorption of absorbate ions or molecules occurs on a homogeneous surface using a limitable number of adsorption sites and the adsorption occurred as monolayer adsorption without any interaction could be occurred between adsorbed ions or molecules [30]. Once an adsorption site is filled by absorbate ions or molecules, no further adsorption can occur at that site. The maximum adsorption of any ions on the adsorbent surface will be achieved when the adsorbent surface reached the saturation point. Also, the Langmuir model assumes uniform energies of adsorption onto the adsorbent surface without any transmigration of the adsorbate ions into the adsorbent [32]. Both nonlinear and linear forms of the Langmuir isotherm model can be expressed as the mentioned in equations 3 and 4, respectively, and the linear form was applied to the experimental data.

$$q_e = \frac{q_m\, bC_e}{1+bC_e} \qquad (3)$$

$$\frac{1}{q_e} = \left(\frac{1}{k_L\, q_m}\right)\frac{1}{C_e} + \frac{1}{q_m} \qquad (4)$$

where q_e is the amount of Cr^{6+} ions adsorbed (mg g^{-1}) at equilibrium, k_L is a constant related to the affinity of adsorption sites (L mg^{-1}), q_m gives the maximum theoretical monolayer adsorption capacity (mg g^{-1}) of CGC and C_e is the equilibrium concentration (mg L^{-1}) of Cr^{6+} ions in solution. The experimental data were plotted as $1/q_e$ against 1/Ce and shown in Fig. 9 for adsorption of Cr^{6+} ions onto CGC. The linear plot in Fig. 9 explained the applicability of Langmuir isotherm model to adsorption of Cr^{6+} onto CGC. Consequently, the occurring of monolayer adsorption of the Cr^{6+} on the surface of the adsorbent CGC is suggested. The values of Langmuir constants were calculated and reported in Table 3. The maximum monolayer capacity, q_m, obtained from Langmuir isotherm was 434.78 mg g^{-1}, which is higher than that obtained from our previous work using the activated carbon prepared from pomegranate husk (35.21 mg g^{-1}) [30] and of the activated carbon obtained from *Casuarina equisetifolia* seed husk (172.40 mg g^{-1}) [15]. Also, the adsorption capacity q_m CGC is about ten times higher than that of the peanut shell activated with phosphoric acid (43.73 mg g^{-1}) [5] and the q_m obtained for its starting material chitosan (40.8 mg g^{-1}) [7].

#: (mg g^{-1})(L $mmol^{-1})^{1/n}$; *: (kJ mol^{-1}).

On controversy of Langmuir model, the Freundlich isotherm model describes multilayer

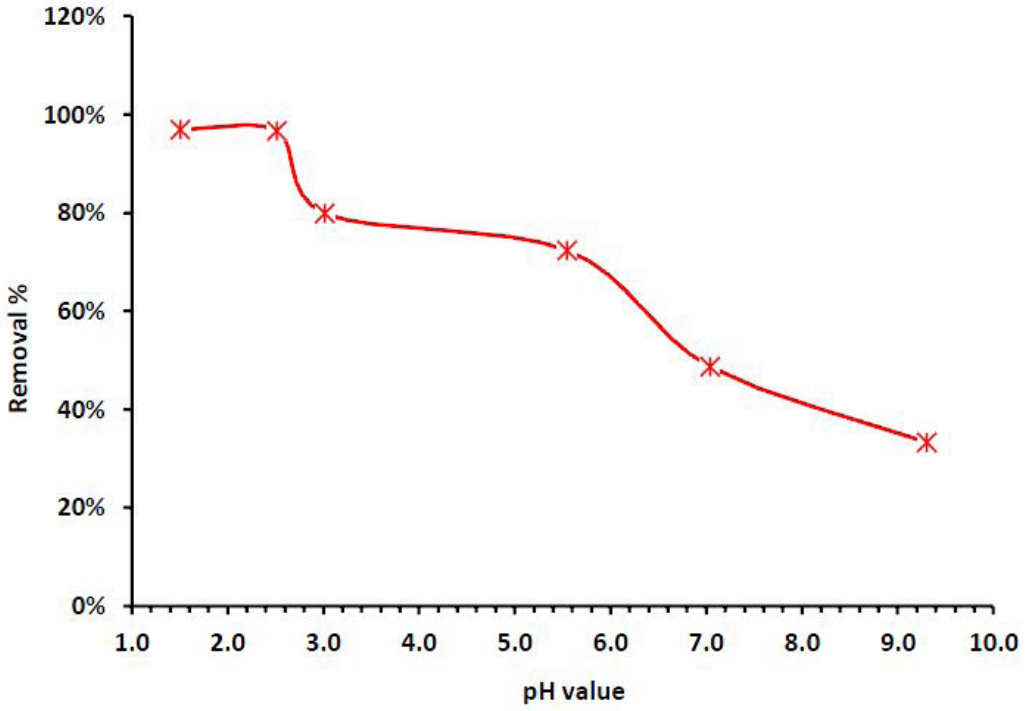

Fig. 6. Effect of system pH on adsorption of chromium (75 mg L^{-1}) onto CGC (250 mg/100 mL) at 25 ± 2 °C at time = 60 min.

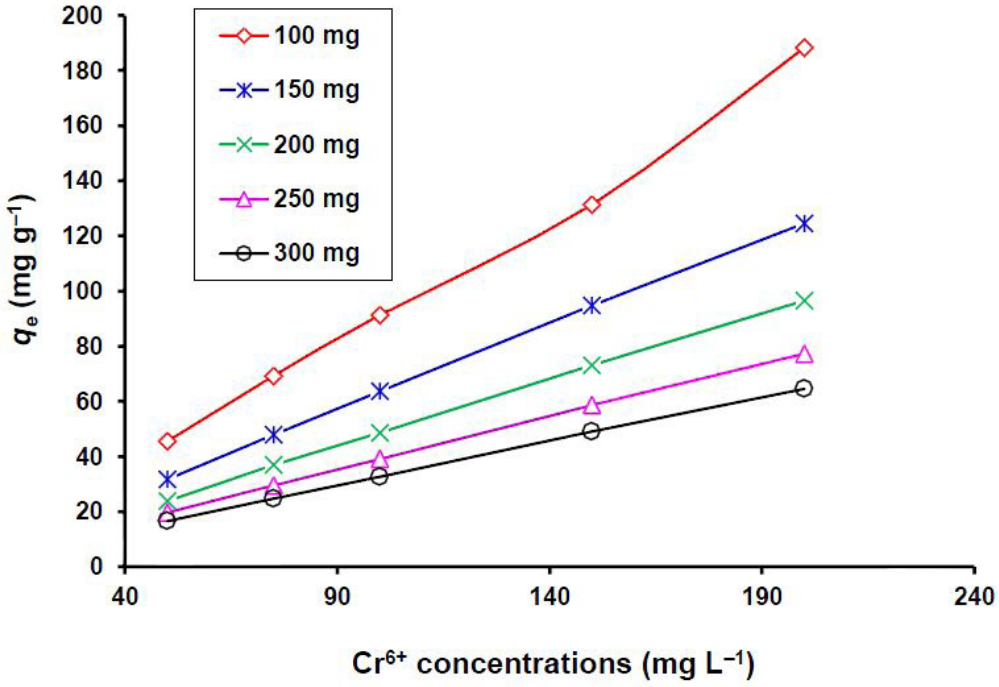

Fig. 7. Relation between amounts of Cr^{6+} ions adsorbed at equilibrium (q_e) and its initial concentration using different CGC doses (0.10 to 0.30 g L^{-1}).

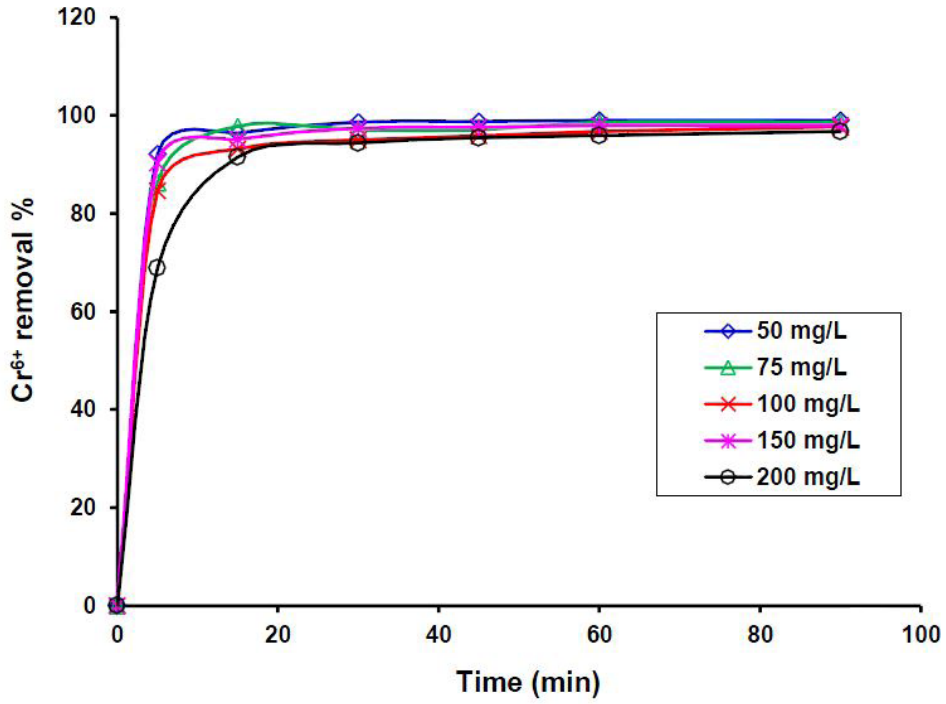

Fig. 8. Effect of contact time on the removal of different initial concentrations of chromium (50 to 200 mg L^{-1}) using CGC (3 g L^{-1}) at pH 1.5.

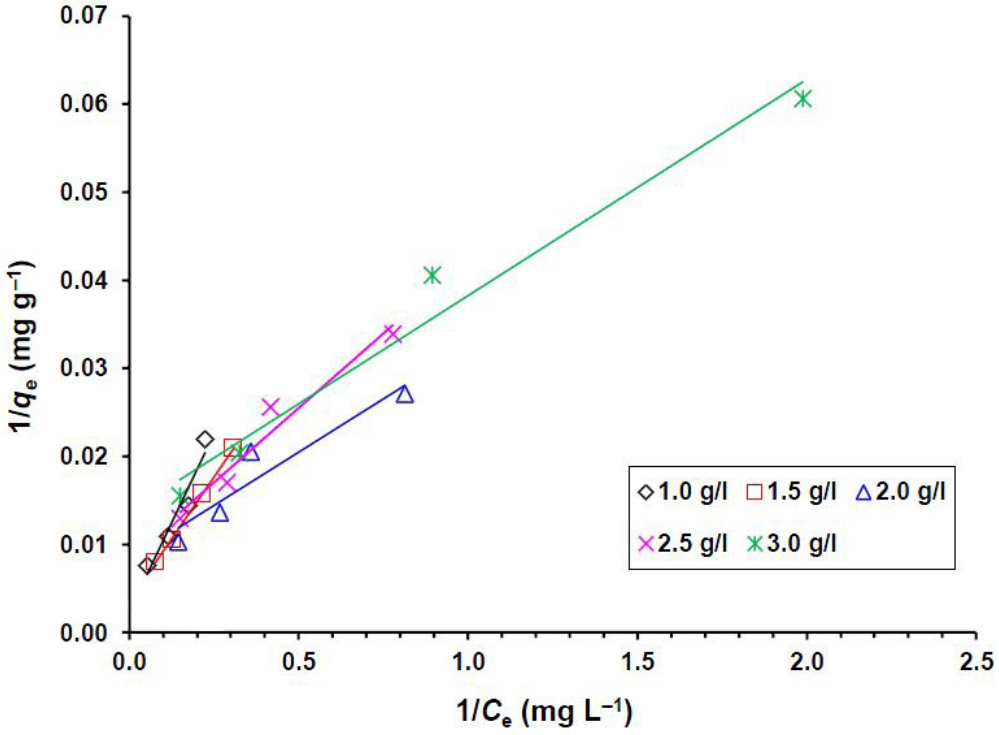

Fig. 9. Langmuir plot for adsorption of Cr^{6+} (100 mg L^{-1}) on CGC (1.0 – 3.0 g L^{-1}) at optimum pH (1.50).

TABLE 1. The amount of catalyst used and the corresponding product yield from 5 g of chitosan.

Catalyst	Product yield (g)	
Amount (mg)	$FeCl_3$	$ZrOCl_2$
300	7.80	6.64
400	7.10	7.10
500	7.23	7.40

TABLE. 2. EDX analysis of CGC before and after the treatment analysis of Cr^{6+} wastewater.

Element	CGC		CGC-Cr^{6+}	
	Wt%	At%	Wt%	At%
C	64.05	72.43	46.49	61.79
O	30.57	25.95	30.40	30.34
Al	0.48	0.24	0.54	0.32
Cl	1.33	0.51	4.70	2.12
Cr	ND	ND	15.78	4.85
Fe	3.56	0.87	2.04	0.58
Co	ND	ND	0.05	0.01

TABLE 3. Isotherm parameters obtained from Langmuir, Freundlich and Tempkin models for the adsorption of Cr^{6+} ions onto CGC.

Model	Parameter	1.0 g L^{-1}	1.5 g L^{-1}	2.0 g L^{-1}	2.5 g L^{-1}	3.0 g L^{-1}
Langmuir	q_m (mg g^{-1})	434.78	277.78	119.04	116.28	72.99
	$k_L \times 10^3$	28.50	64.29	337.37	201.88	561.50
	R^2	0.994	0.999	0.998	0.985	0.984
Freundlich	n	1.45	1.45	1.72	1.64	1.92
	$K_F^{\#}$	18.65	21.84	31.26	24.96	22.93
	R^2	0.927	0.992	0.940	0.967	0.988
Tempkin	B_T	57.99	55.53	35.26	29.43	19.29
	b_T*	0.043	0.045	0.070	0.084	0.128
	Ln (A_T)	–0.63	–0.34	0.69	0.74	1.39
	A_T	5.305	0.714	1.989	2.086	4.030
	R^2	0.988	0.999	0.992	0.999	0.980

adsorption well on an energetically heterogeneous active sites of an adsorbent accompanied by interactions between adsorbed ions or molecules [33]. The equilibrium data were obtained by keeping the initial Cr^{6+} concentrations constant using different adsorbent (CGC) mass at optimum pH for 60 min contact time. Both the Freundlich nonlinear and linear models form are expressed as

$$q_e = K_F C_e^{1/n} \quad (5)$$

$$log(q_e) = log(K_F) + \frac{1}{n} log(C_e) \quad (6)$$

Where K_F (mg g^{-1}) is the adsorption capacity and n is the intensity constant of the adsorbent. The n value provide indication on the adsorption favorability. When the n value lay in the range between 2 and 10, the adsorption process will be favorable. The n value ranged between 1 and 2 represents moderately favorable adsorption, while the n value less than 1 indicates poor adsorption characteristic [34]. The K_F and n constants are calculated from the intercept and slope, respectively, of the linear plot of log (q_e) versus log (C_e) (Fig. 10) and reported in Table 4. The higher K_F values are indicative of favorable adsorption processes, while the n value more than unity has affinity to adsorption [7].

The correlation coefficient (R^2) values obtained from Fig. 10 indicated that the experimental data did not fit very well with the Freundlich isotherm model. The values of n reported in Table 3 are more than unity, which represent that the Cr^{6+} is favorably adsorbed by the prepared CGC [5].

The Tempkin isotherm model is based on the assuming that the adsorption energy decreases linearly with the increase in the surface coverage due to adsorbent-absorbate interactions. Both the non-linear and linear Tempkin isotherm model are described in equations 7 and 8, respectively [35].

$$q_e = \frac{RT}{b} ln(A_T C_e) \quad (7)$$

$$q_e = B_T ln(A_T) + B_T ln(C_e) \quad (8)$$

Where $B_T = (RT)/b$ and A_T (L g^{-1}) are the Tempkin constant and can be determined by a plot of q_e versus ln (C_e) (Fig. 11). T and R (8.314 J mol^{-1} K^{-1}) are the absolute temperature in Kelvin and the universal gas constant, respectively, while b is a constant related to the heat of adsorption. The parameters of Tempkin isotherm model were calculated from Fig. 11 and presented in Table 3.

The correlation coefficients (R^2) values (Table 3) obtained for Tempkin isotherm model proved that the model fitted quite well with the experimental data of the Cr^{6+} adsorption on CGC. The values of b_T in Table 3 showed that the adsorption of Cr^{6+} process onto CGC involved chemisorption since the ion-exchange mechanism involve need the bonding energy (b_T) range to be 8-16 kJ mol^{-1} [5].

Adsorption kinetic studies

Batch adsorption experiment studies were made to explore the Cr^{6+} ions adsorption rate by CGC sample at optimum pH using different Cr^{6+} concentrations and CGC masses. The reaction rate parameters obtained from the kinetic studies are required to determine the optimum operating conditions for the removal batch process. Therefore, the Cr^{6+} ions removal process from water by CGC was investigated with pseudo first-order [36] and pseudo second-order [37] kinetic models. The applicability of these models is weight by the correlation coefficients (R^2 values close or equal to 1.0) and the congruence between the q_e from experimental and q_e calculated from these models [30].

Lagergren [36] reported the pseudo-first-order model as the earliest known equation model to calculate the adsorption rate constant based on the adsorption experimental results. The differential pseudo-first-order model is expressed as equation 9.

$$\frac{dq_t}{dt} = k_1(q_e - q_t) \quad (9)$$

The Lagergren liner equation can be obtained via integrating equation 9 for the boundary conditions $t = 0$ to $t = t$ and $q_t = 0$ to $q_t = q_t$ to give the liner equation 10:

$$log(q_e - q_t) = log(q_e) - \frac{k_1}{2.303} t \quad (10)$$

where q_e (mg g^{-1}), q_t (mg g^{-1}) and k_1 (min^{-1}) are the adsorption capacity at equilibrium, and the adsorption capacity at time t, and rate constant of the pseudo-first order. Plotting of log ($q_e - q_t$) versus t (Fig. 12) expressed the less applicability of pseudo-first order to the adsorption of Cr^{6+} ions by CGC sample since the calculated q_e values do not agree with the experimental q_e values

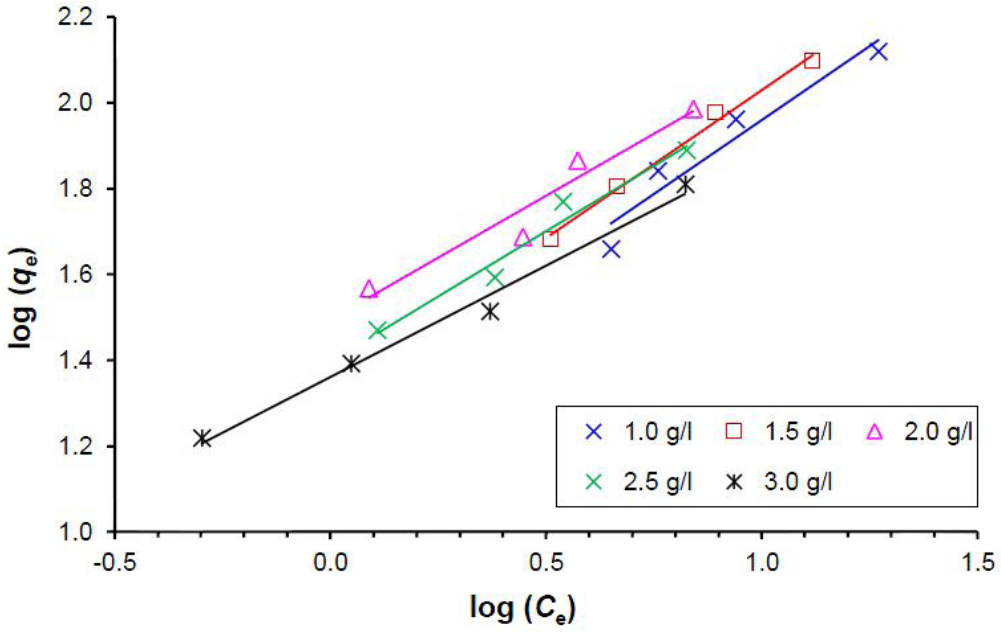

Fig. 10. Freundlich adsorption isotherm for Cr^{6+} (100 mg L^{-1}) adsorption on CGC (1.0 to 3.0 g L^{-1}) at optimum pH.

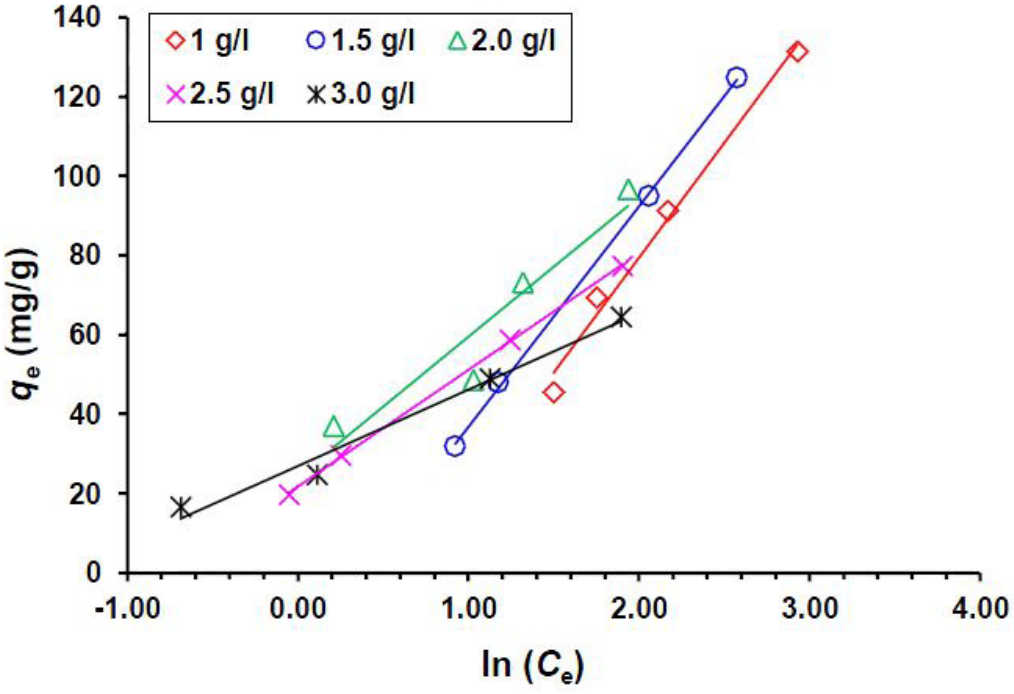

Fig. 11. Tempkin adsorption isotherm for Cr^{6+} (100 mg L^{-1}) adsorption on CGC of different masses (1.0 to 3.0 g L^{-1}) at optimum pH.

TABLE 4. Kinetic parameter for the adsorption of Cr^{6+} ions (50 – 200 mg L^{-1}) onto CGC (1.0 to 3.0 g L^{-1}) at optimum pH (1.5).

Parameter			First-order kinetic model			Second-order kinetic model			
CGC (g L^{-1})	Cr^{+6} (mg l^{-1})	q_e (exp.)	k_1 x 10^3	q_e (calc.)	R^2	k_2 x 10^3	q_e (calc.)	h	R^2
	50	45.53	58.95	17.58	0.950	6.91	47.17	15.38	1.000
	75	69.25	42.15	7.26	0.836	14.82	69.93	72.46	1.000
1.0	100	91.29	74.85	46.83	0.970	3.16	95.24	28.65	1.000
	150	131.34	93.27	111.51	0.880	1.93	136.99	36.23	0.999
	200	188.27	23.49	91.56	0.941	0.55	200.00	22.00	0.987
	50	31.66	90.74	11.07	0.980	20.62	32.26	21.46	1.000
	75	47.84	121.37	44.93	0.897	20.80	48.08	48.08	1.000
1.5	100	63.58	77.38	25.35	0.993	15.30	65.36	65.36	1.000
	150	94.79	101.79	53.33	0.981	10.30	97.09	97.09	0.999
	200	124.58	90.05	101.76	0.968	7.60	131.58	131.58	0.999
	50	23.80	89.36	9.44	0.906	28.62	24.21	16.77	1.000
	75	36.89	77.15	3.66	0.954	47.29	37.17	65.34	1.000
2.0	100	48.60	85.67	9.25	0.966	10.03	50.00	25.08	1.000
	150	73.13	117.91	14.15	0.892	16.88	74.07	92.61	1.000
	200	96.54	97.42	48.21	0.955	5.67	99.61	56.26	1.000
	50	19.62	74.16	2.16	0.809	61.21	19.84	24.09	1.000
	75	29.49	35.01	1.22	0.397	66.81	29.59	58.50	1.000
2.5	100	39.04	12.73	96.96	0.930	19.91	39.68	31.35	1.000
	150	58.62	75.54	8.06	0.953	24.41	59.17	85.46	1.000
	200	77.32	45.83	7.80	0.995	15.75	78.13	96.14	1.000
	50	16.50	16.81	0.42	0.053	163.79	16.58	45.03	1.000
	75	24.63	121.37	5.53	0.650	68.87	24.75	42.19	1.000
3.0	100	32.55	43.07	3.88	0.938	31.11	32.79	33.45	1.000
	150	48.98	90.51	6.27	0.972	0.89	56.18	2.81	0.971
	200	64.45	40.53	5.80	0.982	9.63	65.79	41.68	1.000

even when the correlation coefficient R^2 values are relatively high (Table 4). This indicated that the adsorption capacity alone was not the major factor controlling the adsorption mechanisms of the absorbent [7].

The Cr^{6+} ions adsorption kinetic was then applied to Ho *et al*. [37] pseudo-second-order kinetic model which is given by differential equation 11 [37]. The liner form of pseudo-second-order kinetic model was obtained by integrating equation 11 for the boundary conditions as mentioned above for the pseudo-first order gave the linear equation 12.

$$\frac{dq_t}{dt} = k_2 (q_e - q_t)^2 \qquad (11)$$

$$\frac{t}{q_t} = \frac{1}{k_2 q_e^2} + \frac{1}{q_e} t \qquad (12)$$

Where k_2 (g mg^{-1} min^{-1}) is the second-order rate constant of Cr^{6+} ions adsorption onto CGC sample. The k_2 constant was used to calculate the initial sorption rate (h) by using equation 13.

$$h = k_2 q_e^2 \qquad (13)$$

If the pseudo-second order model is applicable, plot of t/q_t versus t should show a linear relationship. The constant (k_2) and q_e calculated were obtained from the intercept and slope, respectively, of Fig. 13. The q_e calculated values were in good agreement with the q_e experimental values at different initial Cr^{6+} concentrations and CGC masses (Table 6) with correlation coefficients mainly equal to unity, which indicated the good applicability of the pseudo-second-order kinetic model to the adsorption of Cr^{6+} ions onto CGC sample.

Kinetic model proposed by Elovich [30] is generally expressed as the following differential equation 14:

$$\frac{dq_t}{dt} = \alpha exp(-\beta q_t) \qquad (14)$$

where α (mg g^{-1} min^{-1}) and β (g mg^{-1}) are the initial adsorption rate and desorption constant of the experimental process, respectivily. Differential equation 14 was simplified to give equation 15 by assuming $\alpha\beta t >> t$ and by applying the boundary conditions $q_t = 0$ at $t = 0$ and $q_t = q_t$ at $t = t$.

$$q_t = \frac{1}{\beta} ln[\alpha\beta] + \frac{1}{\beta} \ln (t) \qquad (15)$$

If Cr^{6+} adsorption by CGC fits the Elovich model, a plot of q_t where $ln(t)$ should yield a linear relationship with a slope of $(1/\beta)$ and an intercept of $(1/\beta) \times ln(\alpha\beta)$ (Fig. 14). The Elovich constants were calculated from the slope and intercept of the straight line in Fig. 14 and mentioned in Table 5. The correlation coefficients obtained by Elovich equation were lower than that obtained from pseudo-first and second-order models.

The adsorption of molecules or ions onto solid mater (intraparticle diffusion) is a multi-step adsorption that required the transport of the absorbate from its solution to the absorbent surface and then followed by diffusion of absorbate into the interior pores of the absorbent, which is expected to be a slow process, and is therefore, the rate-determining step. The intraparticle diffusion model is explored by equation 16 [30]:

$$q_t = K_{dif} t^{0.5} + C \qquad (16)$$

where C and K_{dif} (mg g^{-1} $min^{-0.5}$) are the intercept and the intraparticle diffusion rate constant, respectively. Plot of q_t against $t^{0.5}$ (Fig. 15) provided a multi-linearity correlation obtained which may be indicates the presence of two or more steps occurred during the adsorption process. The thickness of the boundary layer may be obtained from the value of the intercept C. However the resistance to the external mass transfer increases with the increases of C value. Correlation coefficient (R^2) values reported in Table 5 are ranged between 0.693 and 0.993, confirming that the rate-limiting step is actually the intraparticle diffusion process for some removal processes especially when the R^2 values become close to unity. The linear shape of the plots proved that the intraparticle diffusion played an important role in the uptake of Cr^{6+} ions by CGC. However, the plot of some experiments show low linearity for the adsorption of Cr^{6+} ions by CGC which may indicates that both intraparticle diffusion and surface adsorption are involved in the rate-limiting step. It has been reported [26] that if the intraparticle diffusion is the only rate-limiting step, the street line in the plot of q_t versus $t^{0.5}$ should pass through the origin, which is not the case in this study. Therefore, it may be concluded

TABLE 5. Constant parameters of Elovich and intraparticle diffusion models.

CGC	Chromium	Elovich			intraparticle diffusion		
g L^{-1}	(mg l^{-1})	β	$Ln(\alpha\beta)$	R^2	K_{dif}	C	R^2
	50	0.166	3.45	0.938	0.986	36.933	0.888
	75	0.443	26.30	0.869	0.893	61.555	0.755
1.0	100	0.112	6.01	0.864	2.674	68.965	0.755
	150	0.068	4.62	0.937	5.419	86.310	0.900
	200	0.038	2.36	0.964	10.720	85.217	0.960
	50	0.337	6.64	0.800	1.045	23.484	0.620
	75	0.653	26.80	0.981	0.589	42.759	0.908
1.5	100	0.148	5.32	0.905	2.456	44.096	0.749
	150	0.141	9.12	0.839	2.762	72.110	0.796
	200	0.049	2.04	0.950	7.520	64.492	0.825
	50	0.469	7.15	0.817	0.752	17.906	0.639
	75	0.630	1.92	0.817	0.559	32.564	0.635
2.0	100	0.174	4.47	0.828	2.030	32.882	0.648
	150	0.248	1.41	0.844	1.434	62.028	0.667
	200	0.167	11.90	0.827	2.362	77.059	0.806
	50	0.728	10.40	0.720	0.472	16.024	0.532
	75	0.878	21.90	0.693	0.392	26.386	0.514
2.5	100	0.307	7.97	0.795	1.146	30.151	0.615
	150	0.403	19.60	0.893	0.897	51.542	0.731
	200	0.458	30.90	0.971	0.858	69.974	0.929
	50	2.470	36.70	0.887	0.146	15.358	0.724
	75	1.051	21.20	0.715	0.332	21.996	0.547
3.0	100	0.695	18.40	0.918	0.530	28.139	0.780
	150	0.741	32.30	0.895	0.488	45.132	0.734
	200	0.164	65.50	0.804	2.147	47.573	0.627

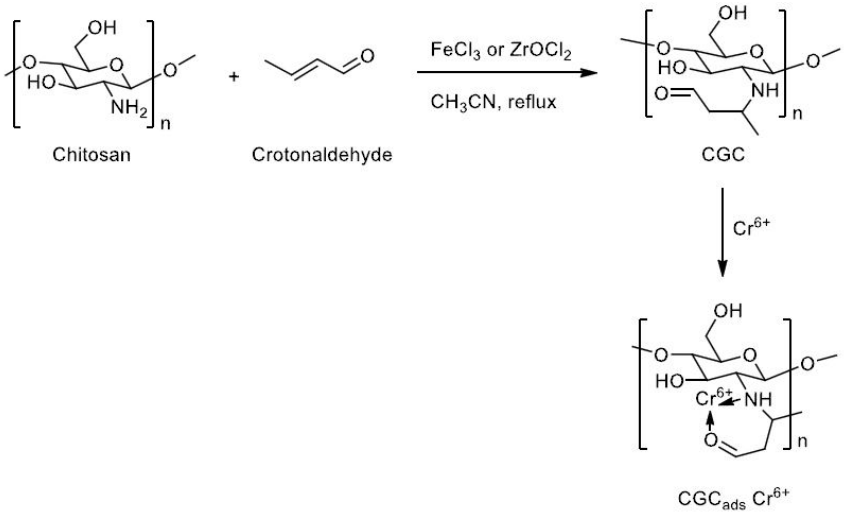

Scheme 1. Synthesis of Chitosan grafted crotonaldehyde (CGC) and its adsorption of hexavalent chromium (Cr^{6+}).

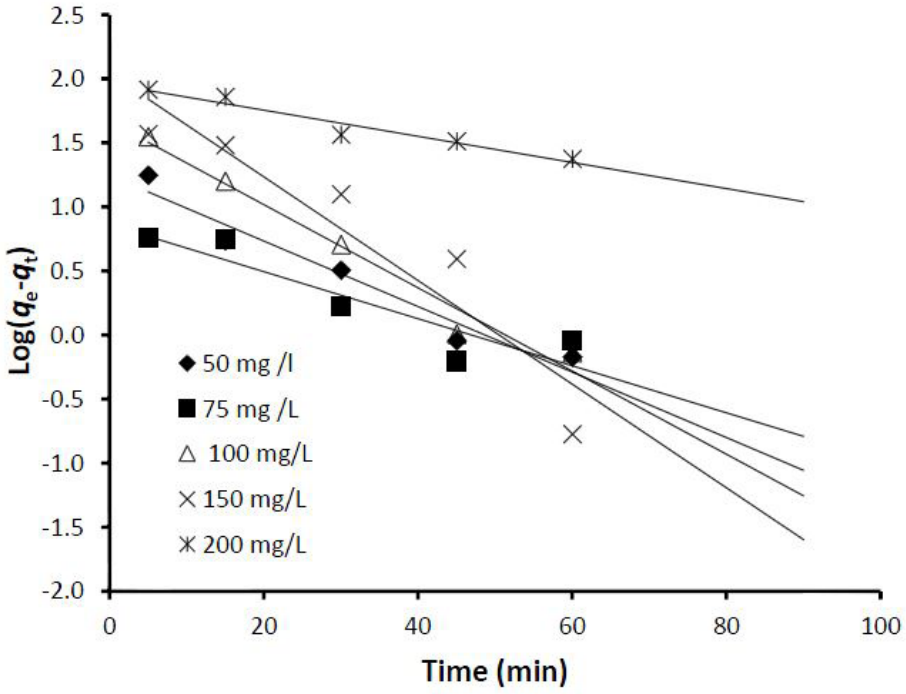

Fig. 12. Plot of the pseudo-first-order at different initial Cr^{6+} ions concentrations (50-200 mg L^{-1}), CGC (1.0 g L^{-1}), pH 1.5 and temperature 25 ± 2 °C.

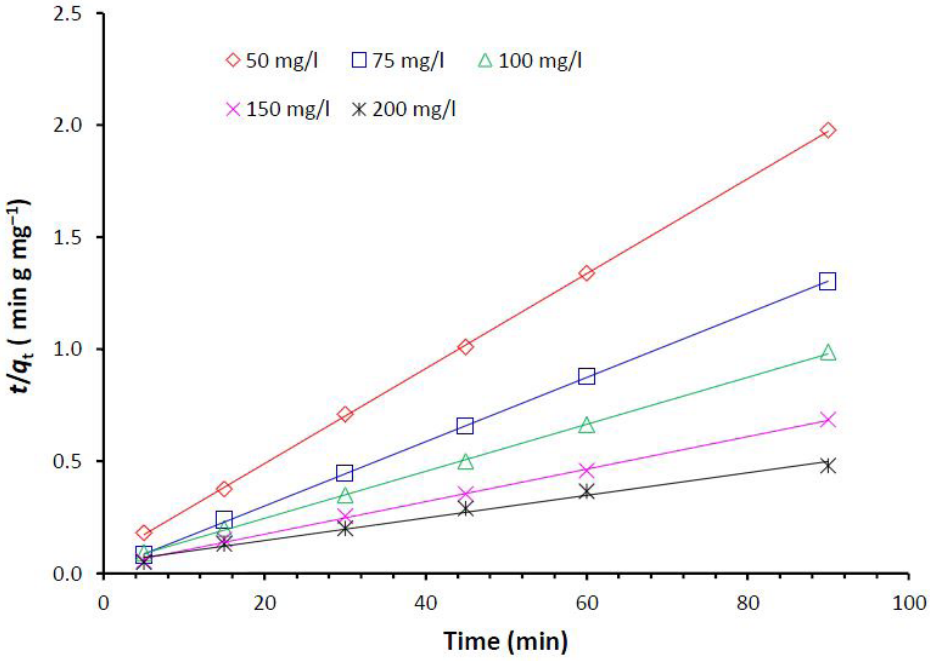

Fig. 13. Plot of the pseudo-second-order at different initial Cr^{6+} ions concentrations (50-200 mg L^{-1}), CGC (1.0 g L^{-1}), pH 1.5 and temperature 25 ± 2 °C.

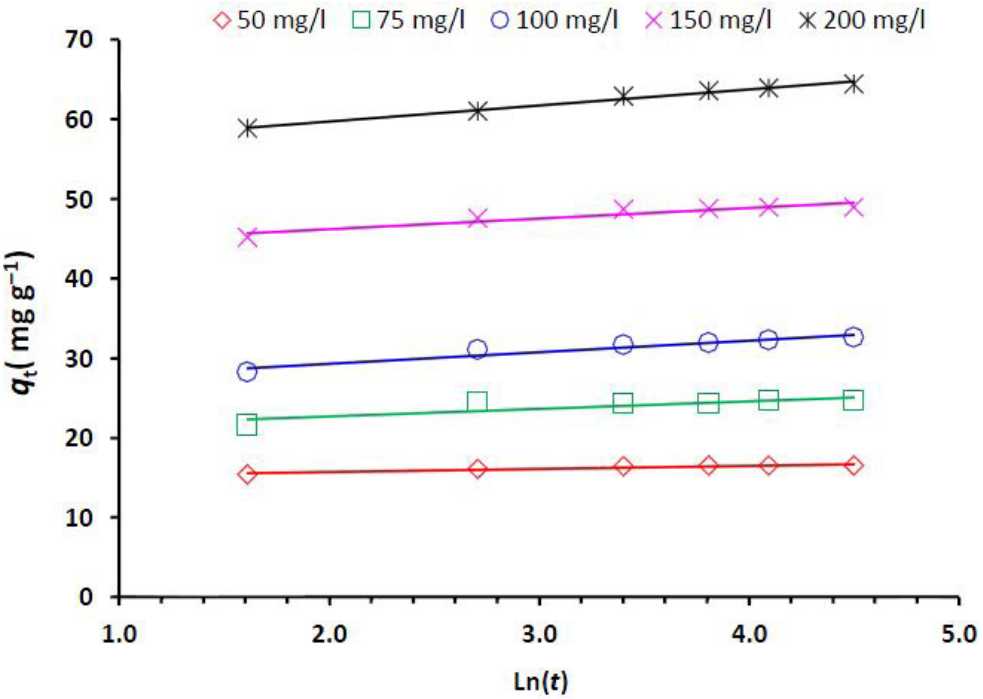

Fig. 14. Elovich model plot for the adsorption of Cr^{6+} ions (50-200 mg L^{-1}) onto CGC (3.0 g L^{-1}).

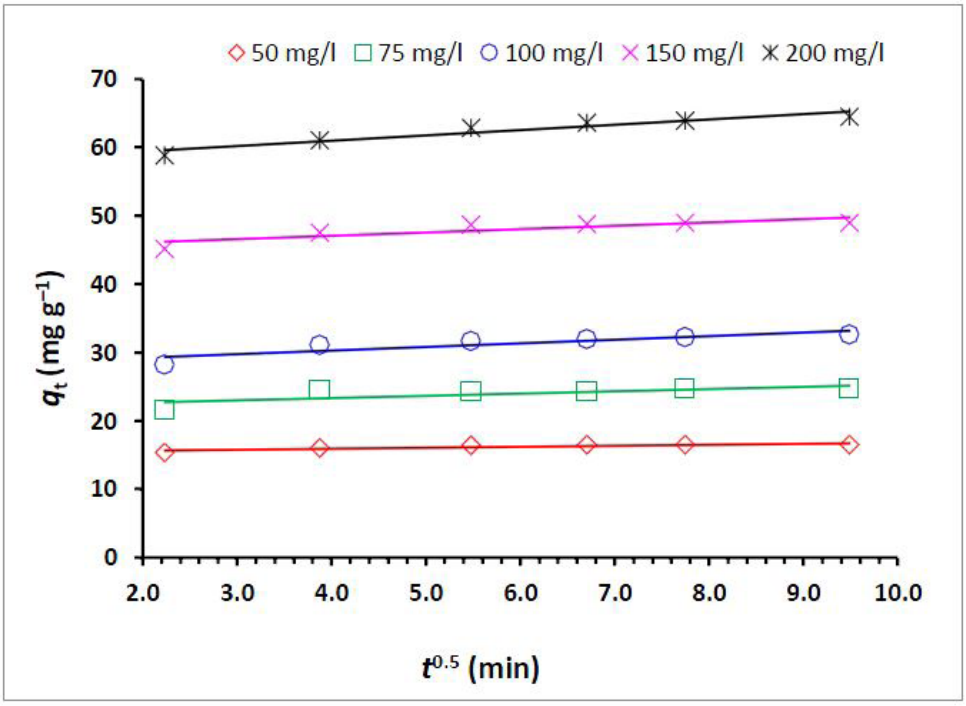

Fig. 15. Intraparticle diffusion model plot for the adsorption of Cr^{6+} (50 – 200 mg L^{-1}) onto CGC (3.0 g L^{-1}) at optimum pH (1.5).

that surface adsorption and intraparticle diffusion were concurrently operating during the Cr^{6+} ions and CGC interactions.

Conclusions

This research involves the synthesis, characterization and application of Chitosan grafting Crotonaldehyde (CGC). The characterization of CGC was explored by various techniques such as TGA, FTIR, EDX and SEM. The applicability of CGC was tested for Cr^{6+} ions removal. The adsorption studies were modeled by Langmuir, Freundlich and Tempkin isotherms. A very high adsorption capacity of 434.78 mg g^{-1} was obtained, which provided a potential application of CGC for toxic Cr^{6+} removal from aqueous solution. A pseudo second-order kinetic model, determined by adsorption capacity and kinetic rate, fitted well for all the adsorbent doses, indicating that chemisorption is dominated the adsorption process. The removal process of Cr^{6+} ions was reported to be controlled by more than one mechanism such as the surface adsorption and intraparticle diffusion. The proposed sorbent (CGC) is efficient, environment friendly and has more than ten times higher in capacity than parent material (chitosan).

References

1. Masoud, A. M.; Saeed, M.; Taha1, M. H.; El-Maadawy, M. M., Uranium adsorption from Bahariya Oasis leach liquor via TOPO impregnated bentonite material; Isothermal, kinetic and thermodynamic studies, *Egyptian Journal of Chemistry,* In press, 2019, DOI: 10.21608/ejchem.2019.13638.1843.

2. Léon, O.; Mũnoz-Bonilla, A.; Soto, D.; Perez, D.; Rangel, M.; Colina, M.; Fernandez-García, M., Removal of anionic and cationic dyes with bioadsorbent oxidized chitosans. *Carbohyd. Poly.* **194**, 375-383 (2018).

3. Saeed, M.; Munir, M.; Khalid, Z.; Ullah, S.; Murtaza, M.; Farid, G.; Rehman, T.; Umar, A.; Elmaadawy, M. M., A review on Functional Dyes on the basis of Design, Development and Hi-tech Applications, *Applied Journal of Environmental Engineering Science,* **5**(1), 99-112 (2019).

4. AL-Othman, Z.A.; Ali, R.; Naushad, Mu., Hexavalent chromium removal from aqueous medium by activated carbon prepared from peanut shell: Adsorption kinetics, equilibrium and thermodynamic studies, *Chem. Eng. J.* **184**, 238–247 (2012).

5. Rai, M. K., et al. "Adsorption of hexavalent chromium from aqueous solution by activated carbon prepared from almond shell: kinetics, equilibrium and thermodynamics study." *Journal of Water Supply: Research and Technology-Aqua* **67**(8), 724-737 (2018).

6. Sun, X.; Yang, L.; Xing, H.; Zhao, J.; Li, X.; Huang, Y.; Liu, H., High capacity adsorption of Cr(VI) from aqueous solution using polyethylenimine-functionalized poly (glycidyl methacrylate) microspheres, *Colloids and Surfaces A: Physicochem. Eng. Aspects*, **457**, 160–168 (2014).

7. Jung, C.; Heo, J.; Han, J.; Her, N.; Lee, S.J.; Oh, J.; Ryu, J.; Yoon, Y., Hexavalent chromium removal by various adsorbents: Powdered activated carbon, chitosan, and single/multi-walled carbon nanotubes, *Separat. Purif. Technol*. **106**, 63–71 (2013).

8. Korus, I.; Loska, K., Removal of Cr(III) and Cr(VI) ions from aqueous solutions by means of polyelectrolyte-enhanced ultrafiltration, *Desalination* **247**, 390–395 (2009).

9. S.S. Kahu, A. Shekhawat, D. Saravanan, R.M. Jugade, Two fold modified chitosan for enhanced adsorption of hexavalentchromium from simulated wastewater and industrial effluents, *Carbohyd. Polym.* **146**, 264–273. (2016).

10. S.A. Mirbagher, S.N. Hosseini b, Pilot plant investigation on petrochemical wastewater treatment for the removal of copper and chromium with the objective of reuse, *Desalination* **171**, 85-93 (2004).

11. Muthukrishnan, M.; Guha, B.K., Effect of pH on rejection of hexavalent chromium by nanofiltration, *Desalination* **219**, 171–178 (2008).

12. Olmez, T., The optimization of Cr(VI) reduction and removal by electrocoagulation using response surface methodology. *J. Hazard. Mater.* **162**, 1371–1378 (2009).

13. Mohan, D.; Singh, K.P.; Singh, V.K., Trivalent chromium removal from wastewater using low cost activated carbon derived from agricultural waste material and activated carbon fabric cloth, *J. Hazard. Mater.* **B135**, 280–295 (2006).

14. Abdelwahab, O.; El Sikaily, A.; Khaled, A.; El Nemr, A., Mass transfer processes of Chromium (VI) adsorption onto Guava seeds, *Chem. Ecol.* **23**(1), 73-85 (2007).

15. El Nemr, A.; El Sikaily, A.; Khaled, A.; Abdelwahab, O., Removal of toxic chromium(VI) from aqueous solution by activated carbon using *Casuarina Equisetifolia*" *Chem. Ecol.* **23**(2), 119-129 (2007)**.**

16. Zhang, L.; Xia, W.; Liu, X.; Zhang, W., Synthesis of titanium cross-linked chitosan composite for efficient adsorption and detoxification of hexavalent chromium from water, *J. Mater. Chem. A,* **3**, 331–340 (2015).

17. El Nemr, A.; Khaled, A.; Abdelwahab, O.; El Sikaily, A., Treatment of wastewater containing toxic chromium using new activated carbon developed from date palm seed, *J. Hazard. Mater.* **152**(1), 263-275 (2008).

18. Wu, M.; Chen, W.; Mao, Q.; Bai, Y.; Ma, H., Facile synthesis of chitosan/gelatin filled with graphene bead adsorbent for orange II removal, *Chem. Eng. Res. Design*. **144**, 35-46 (2019).

19. Sugashini, S.; Begum, K.M.M.S.; Ramalingam, A., Removal of Cr(VI) ions using Fe-loaded chitosan carbonized rice husk composite beads (Fe-CCRCB): Experiment and quantum chemical calculations, *J. Molecular Liquids* **208**, 380–387 (2015).

20. El Sikaily, A.; El Nemr, A.; Khaled, A.; Abdelwahab**,** O., Removal of toxic Chromium from wastewater using green alga *Ulva lactuca* and its activated Carbon, *J. Hazard. Mater.* **148**, 216-228 (2007).

21. El Nemr, A., Pomegranate husk as an adsorbent in the removal of toxic chromium from wastewater, *Chem. Ecol.* **23**(5), 409-425 (2007).

22. Amalraj, A.; Selvi, M. K.; Rajeswari, A.; Christy, E. J. S.; Pius, A., Efficient removal of toxic hexavalent chromium from aqueous solution using threonine doped poly pyrrole nanocomposite, *J. Water Process Eng.* **13**, 88–99 (2016).

23. Sun, X.; Li, Q.; Yang, L.; Liu, H., Chemically modified magnetic chitosan microspheres for Cr(VI) removal from acidic aqueous solution, *Particuology* **26**, 79–86 (2016).

24. Laus, R.; Costa, T.G.; Szpoganicz, B.; Fvere, V.T., Adsorption and desorption of Cu(II), Cd(II) and Pb(II) ions using chitosan crosslinked with epichlorohydrin-triphosphate as the adsorbent, *J. Hazard. Mater.* **183**, 233–241 (2010).

25. Zarghami, Z.; Akbari, A.; Latifi, A.M.; Amani, M.A., Design of a new integrated Chitosan-PAMAM Dendrimer biosorbent for heavy metals removing and study of its adsorption kinetics and thermodynamics, *Biores. Technol.* **205**, 230–238 (2016).

26. El Nemr, A.; Ragab, S.; El Sikaily, A.; Khaled, A., Synthesis of cellulose triacetate from cotton cellulose by using NIS as a catalyst under mild reaction conditions, *Carbohyd. Polym.* **130**, 41–48 (2015).

27. Fatima, A.; Zafar, M.; Ahmad, M.; Yaseen, G.; Sultana, S.; Gulfraz, M.; Khan, A. M., "Scanning electron microscopy as a tool for authentication of oil yielding seed", *Microsc. Res. Tech.* (2018) 1–6. DOI: 10.1002/jemt.23017

28. Munir, M.; Ahmad, M.; Saeed, M.; Waseem, A.; Rehan, M.; Nizami, A.-S.; Zafar, M.; Arshad, M.; Sultana, S., Sustainable production of bioenergy from novel non-edible seed oil (Prunus cerasoides) using bimetallic impregnated montmorillonite clay catalyst, *Renewable and Sustainable Energy Reviews* **109**, 321-332 (2019).

29. Akhtar, M. T.; Ahmad, M.; Shaheen, A.; Zafar, M.; Ullah, R.; Asma, M.; Sultana, S.; Munir, M.; Rashid, N.; Malik, K.; Saeed, M. and Waseem, A., Comparative Study of Liquid Biodiesel From Sterculia foetida (Bottle Tree) Using CuO-CeO_2 and Fe_2O_3 Nano Catalysts, *Frontiers in Energy Research* **7**(4), 1-15 (2019).

30. El Nemr, A., Potential of pomegranate husk carbon for Cr(VI) removal from wastewater: Kinetic and isotherm studies, *J. Hazard. Mater.* **161**, 132–141 (2009).

31. Malkoç, E.; Nuhoglu, Y., The removal of chromium(VI) from synthetic wastewater by Ulothrix zonata, *Fresenius Environ. Bull*. **12** (4), 361–376 (2003).

32. Langmuir, I., The constitution and fundamental properties of solids and liquids, *J. Am. Chem. Soc.* **38**, 2221–2295 (1916).

33. Freundlich, H.M.F., Uber die adsorption in

Losungen, *Zeitschrift fur Physikalische Chemie (Leipzig)* **57A**, 385–470 (1906).

34. Aksu, Z.; Kustal, T.A., Bioseparation process for removing lead(II) ions from waste water treatment by using *C. vulgaris, J. Chem. Technol. Biotechnol.,* **52**, 109-118 (1991).

35. Tempkin, M.J.; Pyzhev, V., Kinetics of ammonia synthesis on promoted iron catalysts. *Acta Physiochimica URSS,* 12, 217-222 (1940).

36. Lagergren, S., Zurtheorie der sogenannten adsorption geloster stoffe, Kungliga Svenska Vetenskapsakademiens, Handlingar, 24, 1–39 (1898).

37. HO, Y.S.; McKay, G.; Wase, D.A.J.; Foster, C. F., Study of the sorption of divalent metal ions on to peat, *Adsorp. Sci. Technol*. **18**, 639–650 (2000).